

Heteronuclear NMR Spectroscopy for Lysine NH₃ Groups in Proteins: Unique Effect of Water Exchange on ¹⁵N Transverse Relaxation

Junji Iwahara, Young-Sang Jung, and G. Marius Clore*

Laboratory of Chemical Physics, National Institute of Diabetes and Digestive and Kidney Disease, National Institutes of Health, Bethesda, Maryland 20892-0520

Received November 21, 2006; E-mail: mariusc@intra.niddk.nih.gov

Abstract: In this paper, we present a series of heteronuclear NMR experiments for the direct observation and characterization of lysine NH₃ groups in proteins. In the context of the HoxD9 homeodomain bound specifically to DNA we were able to directly observe three cross-peaks, arising from lysine NH₃ groups, with ¹⁵N chemical shifts around ~33 ppm at pH 5.8 and 35 °C. Measurement of water-exchange rates and various types of ¹⁵N transverse relaxation rates for these NH₃ groups, reveals that rapid water exchange dominates the ¹⁵N relaxation for antiphase coherence with respect to ¹H through scalar relaxation of the second kind. As a consequence of this phenomenon, ¹⁵N line shapes of NH₃ signals in a conventional ¹H–¹⁵N heteronuclear single quantum coherence (HSQC) correlation experiment are much broader than those of backbone amide groups. A 2D ¹H–¹⁵N correlation experiment that exclusively observes in-phase ¹⁵N transverse coherence (termed HISQC for heteronuclear in-phase single quantum coherence spectroscopy) is independent of scalar relaxation in the *t*₁ (¹⁵N) time domain and as a result exhibits strikingly sharper ¹⁵N line shapes and higher intensities for NH₃ cross-peaks than either HSQC or heteronuclear multiple quantum coherence (HMQC) correlation experiments. Coherence transfer through the relatively small *J*-coupling between ¹⁵Nζ and ¹³Cε (4.7–5.0 Hz) can be achieved with high efficiency by maintaining in-phase ¹⁵N coherence owing to its slow relaxation. With the use of a suite of triple resonance experiments based on the same design principles as the HISQC, all the NH₃ cross-peaks observed in the HISQC spectrum could be assigned to lysines that directly interact with DNA phosphate groups. Selective observation of functional NH₃ groups is feasible because of hydrogen bonding or salt bridges that protect them from rapid water exchange. Finally, we consider the potential use of lysine NH₃ groups as an alternative probe for larger systems as illustrated by data obtained on the 128-kDa enzyme I dimer.

Introduction

Lysine side-chain NH₃ groups have a p*K*_a in the range 9.5–11.0^{1–3} and are positively charged at neutral pH. As a result lysine side chains often play an important role in protein function, particularly with regard to protein–protein and protein–nucleic acid recognition, through the formation of salt bridges with carboxylates of glutamate and aspartate and the phosphate groups of DNA and RNA. NMR characterization, however, of lysine NH₃ groups is challenging primarily because of rapid hydrogen exchange with water.⁵ NH₃ groups with water-exchange rates greater than ~100 s^{–1} are generally undetectable by ¹H NMR. Indeed, Liepinsh and Otting found that the water exchange rate (*k*_{ex}^{water}) for the NH₃ group of free lysine is as fast as 4000 s^{–1} at pH 7.0 and 36 °C.⁴ Nevertheless, depending on the surrounding environment (e.g., the presence of strong

electrostatic interactions), the exchange rates for some lysine NH₃ groups can be slow enough at lower pH and temperature to permit their observation by ¹H NMR.

In principle one would expect that heteronuclear NMR spectroscopy should be useful for characterizing lysine NH₃ groups.⁵ Yet, even when *k*_{ex}^{water} is slow enough to permit their detection by ¹H NMR, cross-peaks corresponding to lysine NH₃ groups are barely visible in a standard ¹H–¹⁵N heteronuclear single quantum coherence (HSQC) correlation experiment optimized for backbone amides which accounts for why so little is known to date about ¹⁵N NMR of NH₃ groups in proteins. The difficulty in observing ¹H–¹⁵N correlations for lysine NH₃ groups is due to two factors: (a) the ¹⁵N chemical shift of lysine NH₃ that resonates ~90 ppm upfield from the backbone ¹⁵N resonances and (b) the unique ¹⁵N transverse relaxation properties of NH₃ groups.

In this paper, we demonstrate that ¹⁵N transverse relaxation for lysine NH₃ groups is highly affected by water exchange through scalar relaxation of the second kind.^{6,7} Although both NH₃ and CH₃ groups are AX₃ spin-systems, this effect is specific

(1) Brown, L. R.; De Marco, A.; Wagner, G.; Wüthrich, K. *Eur. J. Biochem.* **1976**, *62*, 103–107.

(2) Gao, G.; DeRose, E. F.; Kirby, T. W.; London, R. E. *Biochemistry* **2006**, *45*, 1785–1794.

(3) Gao, G.; Prasad, R.; Lodwig, S. N.; Unkefer, C. J.; Beard, W. A.; Wilson, S. H.; London, R. E. *J. Am. Chem. Soc.* **2006**, *128*, 8104–8105.

(4) Liepinsh, E.; Otting, G. *Magn. Reson. Med.* **1996**, *35*, 30–42.

(5) Farmer, B. T., II; Venters, R. A. *J. Biomol. NMR* **1996**, *7*, 59–71.

(6) Abragam, A. *The Principles of Nuclear Magnetism*; Carendon Press: Oxford, 1961; Chapter VIII, p 309.

to NH₃ groups and constitutes a clear distinction to the case of ¹³C transverse relaxation of CH₃ groups. While Kay and co-workers have demonstrated that heteronuclear multiple quantum coherence (HMQC)⁸ spectroscopy represents the best experiment for optimal ¹H–¹³C correlation of CH₃ groups,^{9,10} we demonstrate that neither HSQC¹¹ nor HMQC experiments are ideal for NH₃ groups. In both HSQC and HMQC experiments, scalar relaxation via water exchange results in ¹⁵N line shapes for NH₃ groups that are even broader than those of backbone amide groups, even though fast internal motion should result in significantly slower ¹⁵N relaxation for NH₃ groups. To circumvent this problem we have designed an alternative ¹H–¹⁵N correlation experiment that is completely independent of such scalar relaxation in the ¹⁵N-dimension by forcing the ¹⁵N transverse coherence to always be in-phase with respect to ¹H during the t₁(¹⁵N) evolution period. This experiment which we refer to as HISQC for heteronuclear in-phase single quantum coherence spectroscopy takes full advantage of the intrinsically slow ¹⁵N relaxation of NH₃ groups, resulting in strikingly better resolution and sensitivity over HMQC and HSQC experiments. We also present a suite of triple resonance experiments based on the same principle for assignment of lysine NH₃ resonances. The application of these methods is illustrated for the 22 kDa HOXD9 homeodomain–DNA complex and the 128 kDa enzyme I dimer.

Materials and Methods

NMR Samples. Samples of the 22-kDa complex between ¹³C/¹⁵N- or ²H/¹⁵N-labeled HOXD9 homeodomain and unlabeled 24-bp DNA containing the specific recognition sequence (Shb in ref 12) were prepared as described previously.^{12–14} For Figures 1a, 2, and 3a, the sample was dissolved in buffer comprising 10 mM sodium phosphate (pH 5.8) and 93% ¹H₂O/7% D₂O and placed in Shigemitsu susceptibility-matched microtubes. To avoid undesired NH₂D and NHD₂ species, all other data were recorded using a 270-μl solution of 0.6-mM complex in 10 mM sodium phosphate (pH 5.8) and 100% ¹H₂O sealed in the inner tube of a Shigemitsu external reference coaxial NMR tube (diameters: inner tube, 4.1 mm; outer tube, 5.0 mm). D₂O for the lock signal was placed in a thin layer between the inner and the outer tube (see later).

Full length ¹⁵N-labeled enzyme I (579 amino acid) from *Thermoanaerobacter tengcongensis* was overexpressed in *E. coli* and purified by affinity- and size-exclusion chromatography. A 270-μl solution of 0.4 mM protein dissolved in 20 mM sodium acetate buffer (pH 5.5), 0.1 mM NaN₃, 2 mM DTT and 100% ¹H₂O was sealed in a coaxial tube. Light-scattering data indicated that under these conditions full length enzyme I forms a monodisperse 128-kDa dimer, as reported previously in the literature.¹⁵

NMR Spectroscopy. All NMR experiments except for those reported in Figure 13 were carried out using a Bruker DMX-500 spectrometer equipped with a cryogenic probe (¹H frequency, 500 MHz). Experiments on the HOXD9 homeodomain–DNA complex were carried out at

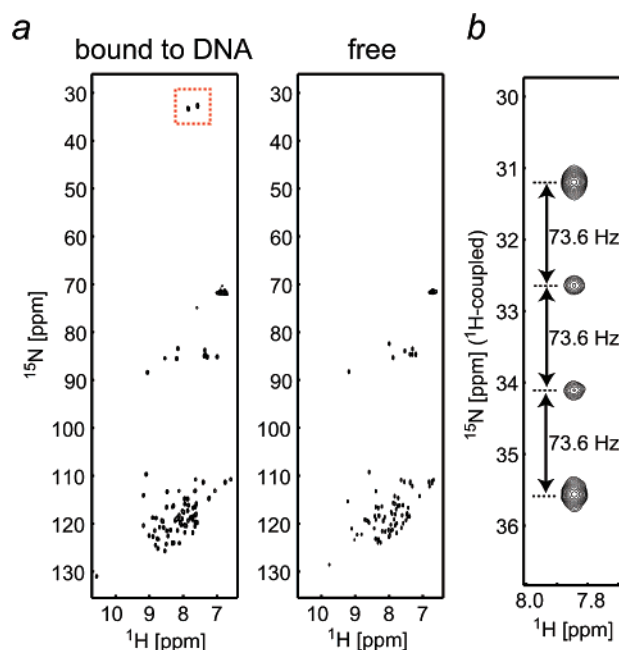


Figure 1. ¹H–¹⁵N HSQC spectra of ¹³C/¹⁵N-labeled HOXD9 homeodomain. (a) 2D ¹H–¹⁵N HSQC spectra measured at pH 5.8 of the homeodomain bound specifically to a 24-bp DNA duplex (left) and in the free state (right). The spectra were recorded at 35 °C with the ¹⁵N-carrier position at 82 ppm and ¹⁵N rf field strengths of 5.2 kHz for 90° and 180° pulses and 1.2 kHz for composite decoupling during acquisition. ¹³C-decoupling was also applied in the ¹⁵N-dimension. The red dashed box indicates the cross-peaks around ~33 ppm that are only observed for the DNA-bound state. (b) Expansion of the F1–¹H-coupled HSQC spectrum showing the signal at 33.3 ppm enclosed within the dashed box in panel a. The quartet structure indicates that the signals arise from NH₃ groups and the value of ¹J_{NH} is 73.6 Hz.

two temperatures (35 and 25 °C). ¹H and ¹⁵N resonances for NH₃ groups were assigned using the suite of triple-resonance experiments shown in Figure 10 along with Lys ¹H/¹³C chemical shifts assigned in our previous studies.^{12–14} Spectra on Enzyme I were recorded on a Bruker DRX-800 spectrometer equipped with a cryogenic probe (¹H frequency, 800 MHz). NMR data were processed using NMRPipe¹⁶ and analyzed with NMRView.¹⁷ Further details of individual NMR experiments are described in the figure captions.

Results and Discussion

HSQC Signals from Lysine NH₃ Groups. The present work was initiated by the observation of cross-peaks with unusual ¹⁵N chemical shifts around 33 ppm observed in the ¹H–¹⁵N HSQC correlation spectrum of ¹³C/¹⁵N-labeled HOXD9 homeodomain complexed to a 24-bp DNA duplex at pH 5.8 and 35 °C (Figure 1a). The corresponding signals were not observed for the free protein under the same conditions, implying that these signals originate from functional groups involved in DNA-binding. In the F1–¹H-coupled HSQC spectrum, the cross-peaks at ~33 ppm exhibit a quartet splitting pattern, indicating that they arise from NH₃ groups (Figure 1b). A similar observation has recently been made for glycoside hydrolase.¹⁸ From the

(7) Bax, A.; Ikura, M.; Kay, L. E.; Torchia, D. A.; Tschudin, R. *J. Magn. Reson.* **1990**, *86*, 304–318.

(8) Bax, A.; Griffey, R. H.; Hawkins, B. L. *J. Magn. Reson.* **1983**, *55*, 301–315.

(9) Tugarinov, V.; Hwang, P. M.; Ollerenshaw, J. E.; Kay, L. E. *J. Am. Chem. Soc.* **2003**, *125*, 10420–10428.

(10) Ollerenshaw, J. E.; Tugarinov, V.; Kay, L. E. *Magn. Reson. Chem.* **2003**, *41*, 843–852.

(11) Bodenhausen, G.; Ruben, D. *J. Chem. Phys. Lett.* **1980**, *69*, 185–189.

(12) Iwahara, J.; Zweckstetter, M.; Clore, G. M. *Proc. Natl. Acad. Sci. U.S.A.* **2006**, *103*, 15062–15067.

(13) Iwahara, J.; Clore, G. M. *J. Am. Chem. Soc.* **2006**, *128*, 404–405.

(14) Iwahara, J.; Clore, G. M. *Nature* **2006**, *440*, 1227–1230.

(15) Patel, H. V.; Vyas, K. A.; Savtchenko, R.; Roseman, S. *J. Biol. Chem.* **2006**, *281*, 17570–17578.

(16) Delaglio, F.; Grzesiek, S.; Vuister, G. W.; Zhu, G.; Pfeifer, J.; Bax, A. *J. Biomol. NMR* **1995**, *6*, 277–293.

(17) Johnson, B. A.; Blevins, R. A. *J. Biomol. NMR* **1994**, *4*, 603–614.

(18) Poon, D. K. Y.; Schubert, M.; Au, J.; Okon, M.; Withers, S. G.; McIntosh, L. P. *J. Am. Chem. Soc.* **2006**, *128*, 15388–15389.

(19) Tjandra, N.; Grzesiek, S.; Bax, A. *J. Am. Chem. Soc.* **1996**, *118*, 6264–6272.

(20) Permi, P. *J. Biomol. NMR* **2002**, *22*, 27–35.

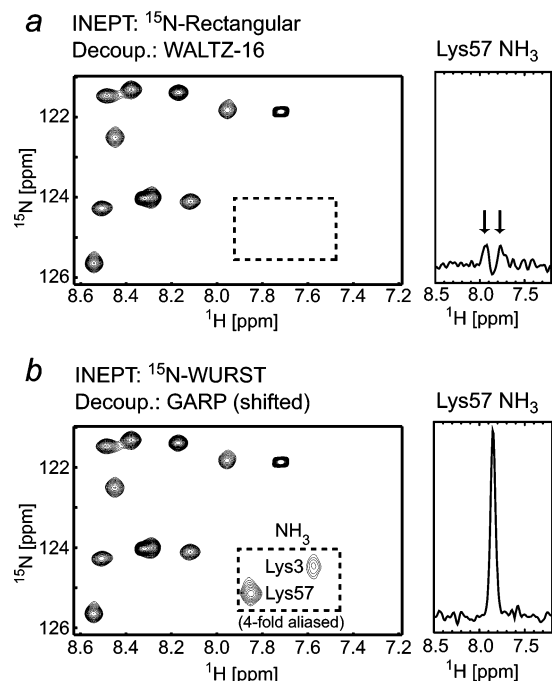


Figure 2. Cross-peaks arising from Lys NH₃ groups in the HOXD9 homeodomain–DNA complex are difficult to observe in standard HSQC experiments for backbone amide groups. (a) HSQC spectrum recorded with ¹⁵N rectangular pulses (rf field strength of 5.2 kHz) with the carrier frequency set to 116 ppm. ¹⁵N-WALTZ-16 decoupling ($\gamma B_1/2\pi = 1.2$ kHz) centered at 116 ppm was applied during acquisition. (b) HSQC spectrum recorded with ¹⁵N WURST inversion pulses (1.25 ms) instead of rectangular 180° pulses. The ¹⁵N carrier frequency was set to 116 ppm for all pulses except the ¹⁵N-GARP ($\gamma B_1/2\pi = 1.2$ kHz) decoupling sequence during acquisition where the carrier was shifted to 80 ppm to ensure effective decoupling over the complete range of ¹⁵N chemical shifts. All other experimental conditions were the same as those for the spectrum shown in panel a. ¹³C-decoupling was applied in the ¹⁵N-dimension. Both spectra were recorded at 35 °C using a Bruker DMX-500 spectrometer at a ¹H-frequency of 500 MHz. The spectral width for the ¹⁵N dimension was 22.9 ppm for each spectrum and the lysine NH₃ cross-peaks are 4-fold aliased. The sample comprised 0.5 mM ¹³C/¹⁵N-labeled HOXD9 homeodomain–DNA complex (pH 5.8). For each panel, a 1D slice along ¹H dimension through the cross-peak of Lys57 NH₃ is also shown (right-hand panels). In the case of the spectrum shown in panel a, the NH₃ cross-peaks are very weak and exhibit doublet splitting (indicated by the arrows).

splitting width of the quartet, the value of the ¹J_{NH} scalar coupling for these NH₃ groups was found to be 73.6 Hz, which is considerably smaller than that for backbone amide groups (~93 Hz; ref 19) or glutamine/asparagine side-chain NH₂ groups (~89 Hz; ref 20). The lower shielding and smaller ¹J_{NH} coupling for NH₃ groups is in accord with the corresponding observations for CH₃ groups for which the ¹³C chemical shift and ¹J_{CH} coupling are both considerably smaller than those for planar sp² CH groups.²¹ The two NH₃ cross-peaks clearly observed in the HSQC experiment were found to originate from Lys3 and Lys57 (see later).

In the standard ¹H–¹⁵N HSQC experiment used for the observation of protein backbone amide groups with the ¹⁵N carrier position around ~116 ppm, the performance of ¹⁵N 180° pulses and composite decoupling schemes are poor for NH₃ signals around ~33 ppm owing to the limited rf strength employed for ¹⁵N (typically ~5.2 kHz for hard pulses; ~1.2 kHz for decoupling), as we found previously for the arginine

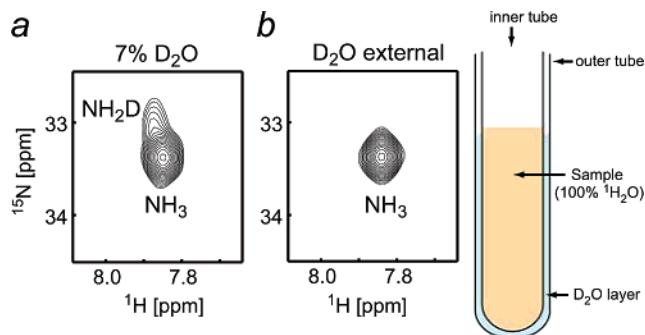


Figure 3. Cross-peak of Lys57 NH₃ in the ¹³C/¹⁵N-HOXD9 homeodomain–DNA complex observed in the HSQC spectrum recorded on samples dissolved in (a) 93% ¹H₂O and 7% D₂O and (b) 100% ¹H₂O. The shoulder of the cross-peak in panel a corresponds to the NH₂D species. In panel b the NMR sample is placed in the inner tube of a coaxial system while D₂O for the NMR lock is located in the external layer between the outer and the inner tubes. The shoulder observed in the cross-peak in panel a is no longer present in the cross-peak in panel b.

side-chain ¹⁵Nε.²² The problem is more severe for NH₃ cross-peaks because of the larger offset (~4.2 kHz at 500 MHz spectrometer). On a 500 MHz spectrometer, application of a rectangular ¹⁵N 180° pulse at 116 ppm with an rf field strength of $\gamma B_1/2\pi = 5.2$ kHz to a magnetization M_0 at 33 ppm along +z results in $M_z = +0.019M_0$ as opposed to $-M_0$. With two INEPT schemes, the signal at 33 ppm is reduced to 24% of the maximum owing to imperfections of the rectangular ¹⁵N 180 pulses. The corresponding values at 600 and 800 MHz are 12% and 1%, respectively. In addition, ¹⁵N-WALTZ decoupling²³ at 116 ppm with $\gamma B_1/2\pi = 1.2$ kHz does not reach 33 ppm even at 500 MHz resulting in doublet splitting and further reduction of the signal intensity. (Note the effective range of the WALTZ-16 decoupling scheme is $\pm 1.2\gamma B_1/2\pi$ in Hz.) Figure 2a shows the NH₃ region of an HSQC spectrum recorded at 500 MHz with the ¹⁵N carrier position at 116 ppm with rf field strengths of 5.2 kHz for hard ¹⁵N pulses and 1.2 kHz for decoupling. As expected from the above considerations, the NH₃ cross-peaks are indeed very weak in this spectrum and doublet splitting in the ¹H dimension is observed. Thus, detection of NH₃ cross-peaks is difficult with a standard HSQC experiment optimized for backbone amide groups at high magnetic field, even if the water-exchange rates are slow enough to permit the observation of NH₃ resonances by ¹H NMR.

Figure 2b shows the HSQC spectrum recorded with broadband ¹⁵N WURST-20 inversion pulses²⁴ for the INEPT transfers, and ¹⁵N-GARP²⁵ centered at 82 ppm for simultaneous decoupling of ¹⁵NH, ¹⁵NH₂, and ¹⁵NH₃. In this HSQC spectrum, the NH₃ cross-peaks are singlets with much higher intensities, while backbone NH cross-peaks are unperturbed relative to a standard HSQC spectrum.

Two features should be noted regarding the NH₃ cross-peaks observed in the HSQC spectrum shown Figure 2b. First, the cross-peaks appear to be asymmetric with broad shoulders located at the upper portion of the NH₃ cross-peaks (Figure 3a). These shoulders correspond to the signals of NH₂D which disappear upon use of a coaxial NMR tube, in which D₂O for the NMR lock signal is placed in a thin outer layer and the

(22) Iwahara, J.; Clore, G. M. *J. Biomol. NMR* **2006**, *36*, 251–257.

(23) Shaka, A. J.; Keeler, J.; Freeman, R. *J. Magn. Reson.* **1983**, *52*, 313–340.

(24) Kupce, E.; Freeman, R. *J. Magn. Reson.* **1995**, *127*, 36–48.

(25) Shaka, A. J.; Keeler, J. *Prog. NMR Spectrosc.* **1987**, *19*, 47–129.

(21) Zwahlen, C.; Legault, P.; Vincent, S. J. F.; Greenblatt, J.; Konrat, R.; Kay, L. E. *J. Am. Chem. Soc.* **1997**, *119*, 6711–6721.

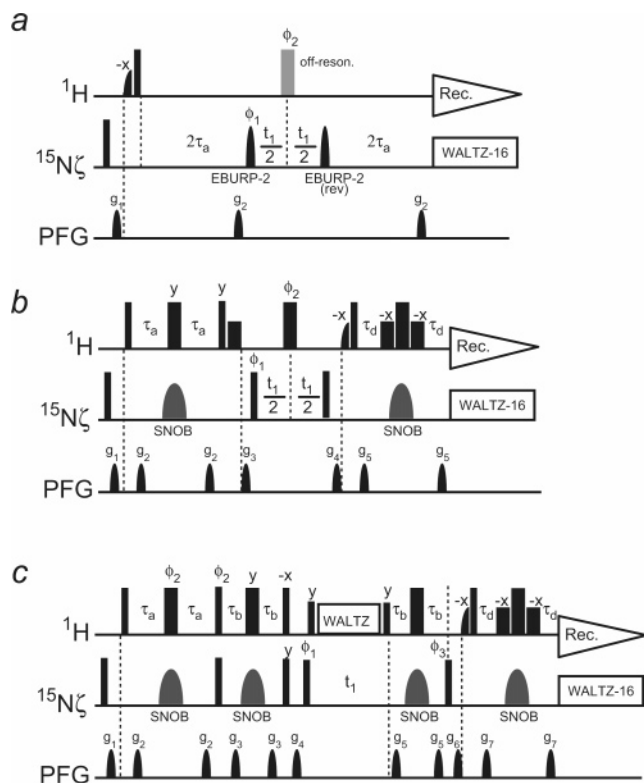


Figure 4. 2D ^1H – ^{15}N correlation experiments for the detection of Lys $^{15}\text{NH}_3$ groups: (a) HMQC, (b) HSQC, and (c) HISQC. Thin and thick bars represent 90° and 180° pulses, respectively. Water-selective half-Gaussian (2.0 ms) and soft-rectangular (1.4 ms) pulses are represented by half-bell and short bold shapes, respectively. A gray bell shape for ^{15}N represents a *r*-SNOB 180° pulse²⁹ (1.03 ms) for inversion and refocusing. Unless indicated otherwise, pulse phases are along *x*. For all pulse sequences, the ^1H carrier position was set at the water resonance and the ^{15}N carrier position at 33 ppm. Rectangular ^{15}N 90° pulses were applied with $\gamma B_1/2\pi = 2.6$ kHz. The delay τ_a was optimized at 2.7 ms, which is considerably shorter than $(4^1J_{\text{NH}})^{-1}$ ($=3.4$ ms) because of the relatively fast ^1H relaxation for NH_3 groups. Quadrature detection in the t_1 domain was achieved using States-TPPI, incrementing the phase ϕ_1 . Field-gradients were optimized to minimize the water signal. (a) The water flip-back HMQC experiment. The gray bar represents an off-resonance ^1H rectangular 180° pulse that does not affect water. EBURP-2 pulses²⁸ (1.6 ms) were applied as $^{15}\text{N}\zeta$ -selective 90° pulses (the second one is time-reversal). Phase cycles: $\phi_1 = \{x, -x\}$; $\phi_2 = \{2x, 2y, 2(-x), 2(-y)\}$; rec. = $\{x, 2(-x), x\}$. (b) The water flip-back HSQC experiment. The delay τ_d is τ_a minus the length of water-selective rectangular 90° pulse. Phase cycles: $\phi_1 = \{x, -x\}$; $\phi_2 = \{2x, 2(-x)\}$; rec. = $\{x, -x\}$. (c) The water flip-back HISQC experiment. The delay τ_b is set to 1.3 ms. To maintain ^{15}N in-phase magnetization, ^1H WALTZ-16 decoupling ($\gamma B_1/2\pi = 3.3$ kHz) is applied along *x* during t_1 in a synchronized mode, sandwiched by additional ^1H 90° pulses along *y* to minimize saturation and dephasing of water magnetization.²⁷ Phase cycles: $\phi_1 = \{y, -y\}$; $\phi_2 = \{2(y), 2(-y)\}$; $\phi_3 = \{4x, 4(-x)\}$; rec. = $\{x, 2(-x), x, -x, 2x, -x\}$. The third ^1H 90° pulse along $-x$ (before the gradient g_4) serves two purposes: it purges unnecessary ^{15}N antiphase magnetization by generating multiple quantum coherence and it flips the water magnetization back to $+z$.

inner tube contains the NMR sample without D_2O to avoid the presence of NH_2D and NHD_2 species (Figure 3b). We therefore used coaxial samples for all subsequent NMR experiments for NH_3 groups. Second, the ^{15}N line widths for the NH_3 cross-peaks in the HSQC spectrum shown in Figure 2b appear broader than those for the backbone NH cross-peaks, although the intrinsic ^{15}N relaxation for an NH_3 group should be much slower than that for an NH group owing to fast rotation about the $\text{N}\zeta\text{—C}\epsilon$ bond. In the following sections, we will address the underlying basis for this observation.

NH_3 Cross-Peaks Exhibit Strikingly Sharper ^{15}N Line Shapes in the HISQC Experiment. We designed three 2-D ^1H – ^{15}N heteronuclear correlation experiments for the selective observation of NH_3 groups: namely, HMQC, HSQC and HISQC (Figure 4, parts a, b, and c, respectively). Since water exchange is rapid for NH_3 groups, each experiment implements a water flip-back scheme^{26,27} for better sensitivity. Although the HISQC experiment is a derivative of the “decoupled HSQC” proposed by Bax and co-workers,⁷ this terminology is not adopted here to avoid confusion. In the HISQC pulse sequence, ^{15}N transverse magnetization during t_1 evolution is forced to always be in-phase (N_x or N_y) with respect to ^1H with continuous use of WALTZ-16 ^1H -decoupling rather than a single 180° pulse. Compared to the HSQC experiment, a NH_3 signal in the HISQC experiment should be scaled down by an additional factor of $3 \cos^4 2\pi^1J_{\text{NH}}\tau_b \sin^2 2\pi^1J_{\text{NH}}\tau_b$ owing to schemes for coherence transfers between $2N_y\text{H}_z$ and N_x . The scaling factor is maximized to be 0.44 by setting $\tau_b = 1.3$ ms for $^1J_{\text{NH}} = 74$ Hz. All three experiments use ^{15}N shaped pulses (EBURP-2 90° pulse²⁸ for the HMQC; and *r*-SNOB 180° pulses²⁹ for the HSQC and HISQC) for selective observation of the ^{15}N signals around 33 ppm.

The spectra recorded with the above three experiments exhibited striking differences. Figure 5 shows NH_3 -selective (a) HMQC, (b) HSQC, and (c) HISQC spectra recorded at 35°C on the $^2\text{H}/^{15}\text{N}$ -labeled HOXD9 homeodomain–DNA complex. All three spectra were recorded with the same number of scans and t_1 time points (140 complex points; $t_1^{\text{max}} = 168$ ms) and processed identically. Peak heights in the HSQC and HMQC spectra are almost identical, but the signals are broader in the HMQC, because of the additional exchange broadening of ^1H transverse magnetization during the t_1 evolution period of the HMQC. (Note that the effect of passive coupling for protons should be negligible because of the use of $^2\text{H}/^{15}\text{N}$ -labeled protein.) Of the three spectra, the HISQC exhibits the highest intensity signals. This may at first appear surprising given that the HISQC experiment suffers from the additional loss of sensitivity as noted above. Further, the line widths in the HISQC spectrum are by far the narrowest of the three spectra. Although the NH_3 signal arising from Lys55 is barely discernible as a small shoulder of the Lys3 cross-peak in the HSQC and HMQC spectra, it is clearly observed as an isolated cross-peak in the HISQC spectrum. This dramatic result suggests that ^{15}N transverse relaxation during t_1 in the HISQC experiment is much slower than that for the HSQC experiment.

Effect of Water Exchange on ^{15}N Transverse Relaxation of the NH_3 Group. To explain the striking difference between the HISQC and HSQC spectra shown in Figure 5, we first discuss various theoretical aspects of ^{15}N relaxation of NH_3 groups. While little is known about the ^{15}N relaxation properties of the NH_3 group, the theory of ^{13}C relaxation for CH_3 groups in macromolecules is well established.^{30–34} Considering that

(26) Grzesiek, S.; Bax, A. *J. Am. Chem. Soc.* **1993**, *115*, 12593–12594.

(27) Kay, L. E.; Xu, G. Y.; Yamazaki, T. *J. Magn. Reson., Ser. A* **1994**, *109*, 129–133.

(28) Geen, H.; Freeman, R. *J. Magn. Reson.* **1991**, *93*, 93–141.

(29) Kupce, E.; Boyd, J.; Campbell, I. D. *J. Magn. Reson., Ser. B* **1995**, *106*, 300–303.

(30) Kay, L. E.; Bull, T. E.; Nicholson, L. K.; Griesinger, C.; Schwalbe, H.; Bax, A.; Torchia, D. A. *J. Magn. Reson.* **1992**, *100*, 538–558.

both NH₃ and CH₃ are AX₃ spin systems and that ¹⁵N chemical shift anisotropy (CSA) for lysine NH₃ measured by solid-state NMR is as small as 15 ppm,³⁵ it is likely that many aspects of the theory of ¹³C relaxation of CH₃ groups is applicable to the ¹⁵N relaxation of lysine NH₃ groups in proteins.

By analogy with the theory of ¹³C relaxation for CH₃ groups, the ¹⁵N transverse relaxation processes for the inner and outer components of the quartet decay as single exponentials with rates R_2^{in} and R_2^{out} , respectively, where $R_2^{\text{in}} < R_2^{\text{out}}$, as a consequence of cross-correlation between three ¹⁵N-¹H dipole-dipole (DD) interactions. In contrast to CSA-DD cross-correlation, ¹⁵N-¹H DD cross-correlation cannot be cancelled out by a ¹H 180° pulse, because this simply swaps two equivalent components (i.e., inner ↔ inner; outer ↔ outer). Under conditions where the spectral density function at zero frequency is dominant, the transverse relaxation rates are given by¹⁰

$$R_2^{\text{in}} = R_2^{\text{slow}} + \frac{3}{2} R_{\text{sc}} \quad (1)$$

$$R_2^{\text{out}} = R_2^{\text{fast}} + \frac{3}{2} R_{\text{sc}} \quad (2)$$

$$R_2^{\text{slow}} = \frac{1}{45} \left(\frac{\mu_0}{4\pi} \right)^2 S_{\text{axis}}^2 \gamma_{\text{H}}^2 \gamma_{\text{N}}^2 \hbar^2 \frac{1}{r_{\text{NH}}^6} \tau_r \quad (3)$$

$$R_2^{\text{fast}} = 9R_2^{\text{slow}} = \frac{1}{5} \left(\frac{\mu_0}{4\pi} \right)^2 S_{\text{axis}}^2 \gamma_{\text{H}}^2 \gamma_{\text{N}}^2 \hbar^2 \frac{1}{r_{\text{NH}}^6} \tau_r \quad (4)$$

where R_2^{slow} and R_2^{fast} are the intrinsic ¹⁵N relaxation rates for the inner and outer components; R_{sc} is the rate for scalar relaxation of the second kind^{6,7} arising from one ¹H nucleus of the NH₃ group (the coefficient of $3/2$ in front of R_{sc} in eqs 1 and 2 arises from an average over contributions from coherence terms such as N_x , $2N_yH_z$, $4N_xH_zH_z$, and $8N_yH_zH_zH_z$ that interconvert rapidly because of $^1J_{\text{NH}}$ evolution); S_{axis}^2 is a generalized order parameter³⁶ for the symmetry axis of the NH₃ group; and τ_r is the rotational correlation time of the macromolecule. In the case of the HOXD9 homeodomain–DNA complex, τ_r was determined to be 11.7 ns at 35 °C from analysis of backbone ¹⁵N relaxation data, which predicts values of $R_2^{\text{slow}} = 0.94 \text{ s}^{-1}$ and $R_2^{\text{fast}} = 8.5 \text{ s}^{-1}$ for an NH₃ group with $S_{\text{axis}}^2 = 0.8$.

The scalar relaxation term R_{sc} arises from autorelaxation of longitudinal magnetization of the coupled ¹H nucleus through mechanisms other than interactions within the spin-system. In the case of a CH₃ group, the sole source of R_{sc} is considered to be ¹H–¹H DD interactions with external ¹H nuclei. The biggest difference between CH₃ and NH₃ spin systems is the presence of water exchange for the NH₃ group. Just as Grzesiek and Bax³⁷ considered for the case of a $2N_zH_z$ term for a NH system, R_{sc}

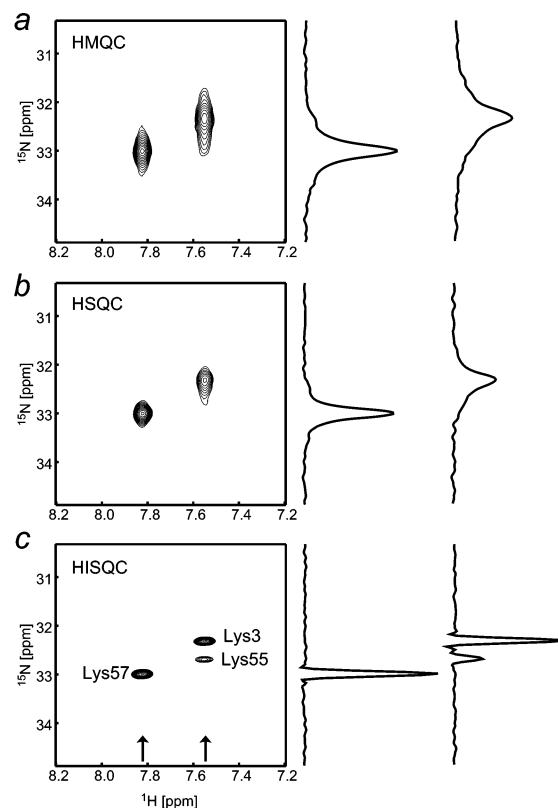


Figure 5. 2D ¹H–¹⁵N correlation spectra recorded at 35 °C on the ²H/¹⁵N-HOXD9 homeodomain–DNA complex (pH 5.8) using the pulse sequences shown in Figure 4: (a) HMQC, (b) HSQC, and (c) HISQC. For each spectrum, the ¹⁵N-dimension was acquired with 140 complex points ($t_1^{\text{max}} = 168 \text{ ms}$) and 8 scans per FID were accumulated. Data were processed identically, applying a 30°-shifted squared cosine-bell window function followed by zero-filling to 512 points for the ¹⁵N dimension. F1-slices at the positions indicated by the arrows are shown. Contour levels and scaling of the slices are identical for all panels.

for a NH₃ group should include the contribution from water exchange and be given by

$$R_{\text{sc}} = \rho_{\text{HH}} + k_{\text{ex}}^{\text{water}} \quad (5)$$

where ρ_{HH} represents the rate for DD interactions with external ¹H nuclei and $k_{\text{ex}}^{\text{water}}$ is the water-exchange rate.

To experimentally investigate the properties of ¹⁵N transverse relaxation for NH₃ groups and the contribution of scalar relaxation, we analyzed the line shapes of the NH₃ quartet in F1–¹H-coupled HSQC spectra measured at 35 and 25 °C on the ²H/¹⁵N-HOXD9 homeodomain–DNA complex (Figure 6). The ¹⁵N-slices (black) are taken from spectra processed with no window function in the ¹⁵N dimension. The NH₃ cross-peak of Lys57 is the only NH₃ cross-peak that exhibits an isolated analyzable quartet (see Figure 5). In the F1–¹H-coupled HSQC experiment, not only the $2N_yH_z^a \rightarrow 2N_yH_z^b$ process but also the $2N_yH_z^a \rightarrow 2N_yH_z^c$ and $2N_yH_z^b \rightarrow 2N_yH_z^c$ coherence transfers occurring during the t_1 -evolution period generate observable

(31) Nicholson, L. K.; Kay, L. E.; Baldisseri, D. M.; Arango, J.; Young, E. P.; Bax, A.; Torchia, A. *Biochemistry* **1992**, *31*, 5253–5263.
 (32) Werbelow, L. G.; Grant, D. M. *J. Chem. Phys.* **1975**, *63*, 4742–4749.
 (33) Kay, L. E.; Torchia, D. A. *J. Magn. Reson.* **1991**, *95*, 536–547.

(34) Palmer, A. G.; Hochstrasser, R. A.; Millar, D. P.; Rance, M.; Wright, P. E. *J. Am. Chem. Soc.* **1993**, *115*, 6333–6345.
 (35) Sarkar, S. K.; Hiyama, Y.; Niu, C. H.; Young, P. E.; Gerig, P. E.; Gerig, J. T.; Torchia, D. A. *Biochemistry* **1987**, *26*, 6793–6800.
 (36) Lipari, G.; Szabo, A. *J. Am. Chem. Soc.* **1982**, *104*, 4546–4559.
 (37) Grzesiek, S.; Bax, A. *J. Biomol. NMR* **1993**, *3*, 627–638.

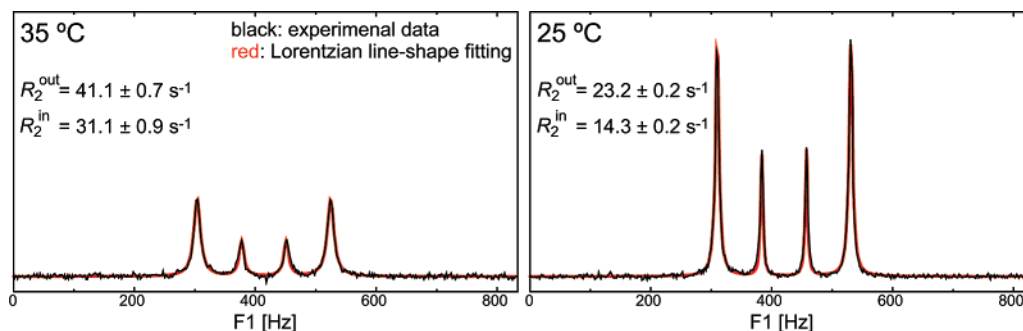


Figure 6. Lorentzian line shape fitting of F1 slices taken from the F1–¹H-coupled HSQC spectra recorded on the ²H/¹⁵N-HOXD9 homeodomain–DNA complex (pH 5.8). The experimental data for Lys57 NH₃ at 35 °C (left) and 25 °C (right) are shown in black. The red lines represent the best fit traces obtained by nonlinear least-squares Lorentzian line shape fitting against the experimental data, using eq 7. The pulse sequence used to record the spectra was similar to that shown in Figure 4b, but lacks the ¹H 180° pulse in the middle of t₁-evolution period and the phase of the initial water-selective 90° pulse was changed to –x for water flip-back. Experimental data were recorded with t₁^{max} = 269 ms and no window function was applied to the ¹⁵N-dimension in data processing. Relaxation rates for the inner and outer components of the ¹⁵N quartet derived from the fitting procedure are also shown.

Table 1. Summary of ¹⁵N Transverse Relaxation and Water-Exchange Rates for the NH₃ Group of Lys57^a

rates (s ⁻¹)	35 °C	25 °C
R ₂ ⁱⁿ ^b	31.1 ± 0.9	14.3 ± 0.2
R ₂ ^{out} ^b	41.1 ± 0.7	23.2 ± 0.2
R ₂ ^{slow} ^c	1.3 ± 0.1	1.1 ± 0.1
R ₂ ^{fast} ^c	11.4 ± 1.2	10.0 ± 0.3
R _{sc} ^c	19.9 ± 0.7	8.8 ± 0.2
k _{ex} ^{water} ^d	18.7 ± 0.3	6.9 ± 0.3
0.25R ₂ ^{fast} + 0.75R ₂ ^{slow} ^e	3.8 ± 0.3	3.3 ± 0.1
R ₂ ^{app} (N _i) ^f	4.5 ± 0.2	4.4 ± 0.1

^a Symbols are as defined in eqs 1–5. ^b From Lorentzian line shape fitting against the quartet in the F1–¹H-coupled HSQC. ^c From R₂ⁱⁿ and R₂^{out} with the constraint that R₂^{fast} = 9R₂^{slow}. ^d From CLEANEX-HISQC experiment. ^e Corresponds to the initial rate for the in-phase term (no scalar relaxation).³³ ^f From relaxation measurements shown in Figure 8.

magnetization. Thus, modulation of the antiphase ¹⁵N term by ¹J_{NH} and chemical shift evolution is given by

$$\begin{aligned}
 &(\cos^3 \pi^1 J_{\text{NH}} t_1 - 2 \sin^2 \pi^1 J_{\text{NH}} t_1 \cos \pi^1 J_{\text{NH}} t_1) \cos \Omega t_1 = \\
 &\frac{3}{8} \cos(\Omega - 3\pi^1 J_{\text{NH}}) t_1 + \frac{1}{8} \cos(\Omega - \pi^1 J_{\text{NH}}) t_1 + \\
 &\frac{1}{8} \cos(\Omega + \pi^1 J_{\text{NH}}) t_1 + \frac{3}{8} \cos(\Omega + 3\pi^1 J_{\text{NH}}) t_1 \quad (6)
 \end{aligned}$$

resulting in a 3:1:1:3 quartet structure providing the relaxation properties of each component of the quartet are the same. Assuming that the inner and outer components of the quartet decay in a single-exponential manner with rate constants R₂^{out} and R₂ⁱⁿ, respectively, the line shape of the quartet is given by

$$\begin{aligned}
 A(\nu) = &\frac{3aR_2^{\text{out}}}{R_2^{\text{out}^2} + 4\pi^2(\nu_0 - \nu)^2} + \frac{aR_2^{\text{in}}}{R_2^{\text{in}^2} + 4\pi^2(\nu_0 + {}^1J_{\text{NH}} - \nu)^2} + \\
 &\frac{aR_2^{\text{in}}}{R_2^{\text{in}^2} + 4\pi^2(\nu_0 + 2{}^1J_{\text{NH}} - \nu)^2} + \frac{3aR_2^{\text{out}}}{R_2^{\text{out}^2} + 4\pi^2(\nu_0 + 3{}^1J_{\text{NH}} - \nu)^2} \quad (7)
 \end{aligned}$$

where ν is the frequency in Hz, ν_0 is the peak position of the lowest frequency component, and a is a scaling factor. The red lines in Figure 6 were obtained by nonlinear least-squares fitting, optimizing the five parameters in eq 7: R₂ⁱⁿ, R₂^{out}, a , ν_0 , and ¹J_{NH}. The calculated curves are in excellent agreement with the

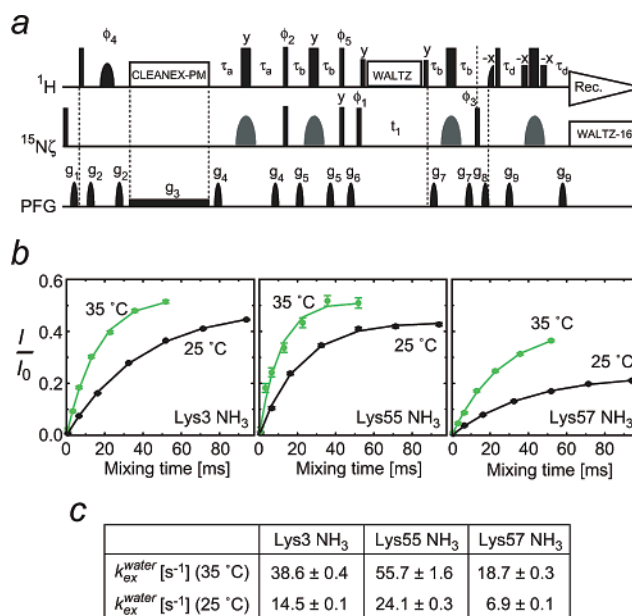


Figure 7. Measurement of water exchange rates for Lys NH₃ groups. (a) CLEANEX-HISQC pulse sequence to measure water exchange rates for Lys NH₃ groups. The CLEANEX component was implemented as described previously.^{38,39} Phase cycles: $\phi_1 = \{y, -y\}$; $\phi_2 = y$; $\phi_3 = \{4x, 4(-x)\}$; $\phi_4 = \{2y, 2x\}$; $\phi_5 = \{2(-x), 2x\}$; rec. = $\{x, 2(-x), x, -x, 2x, -x\}$. The other experimental conditions are the same as those for Figure 4c. (b) Buildup curves for signals arising from exchange between water and lysine NH₃ at 35 °C (green) and 25 °C (black). Seven time-points were used for each measurement. The vertical axis represents the ratio of I to I_0 , where I is the signal intensity observed in the CLEANEX-HISQC and I_0 is that in the reference HSQC (Figure 4c). (c) Values of k_{ex}^{water} exchange rates at 35 and 25 °C.

experimental data, indicating that the individual components of the quartet do indeed decay in a single-exponential manner resulting in Lorentzian line shapes. The values of the relaxation rates obtained in this manner are as follows: R₂^{out} = 41.1 ± 0.7 s⁻¹ and R₂ⁱⁿ = 31.1 ± 0.9 s⁻¹ at 35 °C; R₂^{out} = 23.2 ± 0.2 s⁻¹ and R₂ⁱⁿ = 14.1 ± 0.2 s⁻¹ at 25 °C. It should be noted that the relaxation rates at 25 °C are significantly slower than those at 35 °C, although one might expect the opposite result owing to the increased τ_r at the lower temperature. Assuming that the relationship R₂^{fast} = 9R₂^{slow} is valid, we obtain values of R₂^{slow}, R₂^{fast} and R_{sc} from the experimental R₂ⁱⁿ and R₂^{out} rates using eqs 1 and 2, as shown in Table 1.

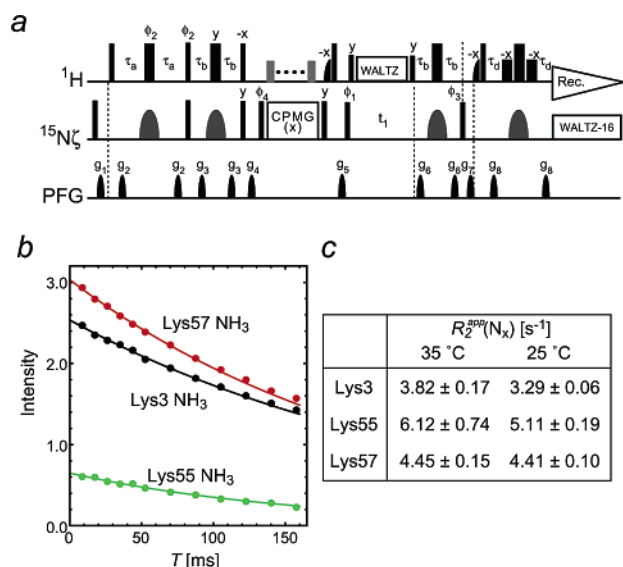


Figure 8. ¹⁵N transverse relaxation for the in-phase N_x term. (a) Pulse sequence used to measure ¹⁵N R_2 rates for N_x of NH₃. For the CPMG pulse train, rectangular ¹⁵N 180° pulses were applied along x with $\gamma B_1/2\pi = 2.6$ kHz. Although not essential for NH₃ because of small CSA, a semiselective ¹H 180° pulse that does not affect the water magnetization was applied once every 4 ms during the CPMG scheme to suppress CSA-DD cross-correlations. Phase cycles: $\phi_4 = \{8y, 8(-y)\}$, rec. = $\{x, 2(-x), x, -x, 2x, -x, -x, 2x, -x, x, 2(-x), x\}$. The other experimental conditions are the same as those in Figure 4c. As Kay et al. pointed out for the case of a CH₃ group,³⁰ the apparent R_2 rates for N_x of a NH₃ group will be affected by the delay τ_b , since a_{in} and a_{out} in eq 8 depend on τ_b . Here, the delay τ_b was set to the same value as that used in the HISQC pulse sequence shown in Figure 4c, since our purpose was to investigate ¹⁵N transverse relaxation properties in the context of the HISQC experiment. (b) ¹⁵N transverse relaxation decay for N_x observed at 35 °C. The measurements were carried out using the ²H/¹⁵N-labeled HOXD9 homeodomain–DNA complex (pH 5.8). (c) Apparent ¹⁵N R_2 rates for lysine NH₃ groups obtained at 35 °C and 25 °C. Since ¹⁵N transverse relaxation for a NH₃ group is expected to be biexponential, the values obtained are meaningful only in a phenomenological sense (see main text). These values are determined using single-exponential fitting against the initial (first 72 ms) portion of the experimental decays, and the curves depicted as solid lines in part b are those calculated from this fitting procedure.

From the above analysis, the scalar relaxation rate R_{sc} was found to be highly sensitive to temperature (19.9 ± 0.7 s⁻¹ at 35 °C versus 8.8 ± 0.15 s⁻¹ at 25 °C), whereas R_2^{slow} and R_2^{fast} were insensitive. The temperature-dependence of R_2^{in} (or R_2^{out}) is primarily due to that of R_{sc} . Further, the contribution of the scalar relaxation term ($1.5R_{\text{sc}}$) to R_2^{in} and R_2^{out} is very large: 96% and 73%, respectively, at 35 °C (92% and 57%, respectively, at 25 °C). Thus, R_2^{in} and R_2^{out} are dominated by scalar relaxation.

Given the temperature-dependence of R_{sc} , it is likely that the water-exchange rate $k_{\text{ex}}^{\text{water}}$ in eq 5 contributes significantly to R_{sc} , particularly in the present case of a deuterated protein for which ρ_{HH} is small (< 1 s⁻¹).⁹ We analyzed water-exchange rates for lysine NH₃ groups using the pulse sequence shown in Figure 7. This experiment makes use of the CLEANEX-PM scheme^{38,39} followed by the HISQC sequence. The values of the $k_{\text{ex}}^{\text{water}}$ rates were calculated from the buildup curves (Figure 7b,c). For the

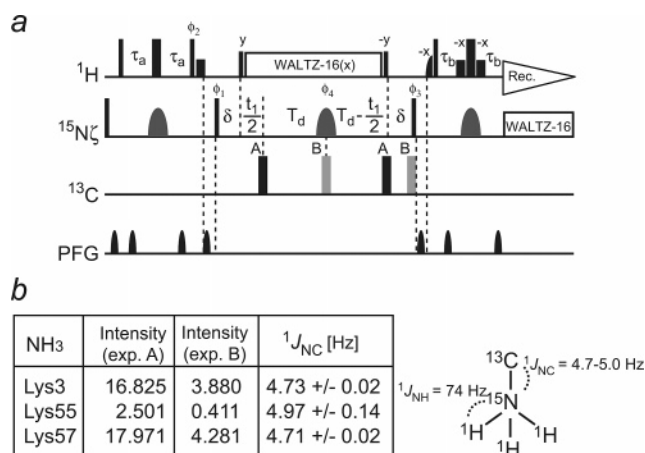


Figure 9. One bond $^1J_{\text{NC}}$ scalar coupling between ¹⁵N ζ and ¹³C ϵ nuclei in Lys residues. (a) The spin-echo difference constant-time 2D ¹H–¹⁵N correlation experiment used for the measurement of $^1J_{\text{NC}\zeta\epsilon}$ couplings. The delays δ and T_d were set to 2.6 and 42.4 ms, respectively. Phase cycles: $\phi_1 = \{x, -x\}$; $\phi_2 = y$; $\phi_3 = x$; $\phi_4 = \{2x, 2y, 2(-x), 2(-y)\}$; rec. = $\{x, -x, -x, x\}$. Other experimental conditions are the same as those for Figure 4c. Two subexperiments A and B (with ¹³C 180° pulses at the indicated positions) were carried out in an interleaved manner. $^1J_{\text{NC}}$ can be calculated from $I_B/I_A = \cos\{\pi^1J_{\text{NC}}(2\delta + 2T_d)\}$, where I_A and I_B are peak intensities in subexperiments A and B, respectively. (b) Measured $^1J_{\text{NC}}$ values for the NH₃ groups of Lys3, Lys55, and Lys57.

NH₃ group of Lys57, the values were 18.7 ± 0.3 s⁻¹ at 35 °C and 6.9 ± 0.3 s⁻¹ at 25 °C, which are only slightly smaller than the values of R_{sc} at the corresponding temperatures (cf. Table 1). Thus, we can conclude that water exchange constitutes the dominant contribution to R_2^{in} and R_2^{out} for ¹⁵N transverse magnetization of NH₃ groups.

On the basis of the above experimental data, we can now explain why the HISQC experiment is far superior to the HSQC experiment with respect to the observation of ¹H–¹⁵N correlations for NH₃ groups (cf. Figure 5): specifically the dramatic difference between the two spectra can be directly attributed to the impact of rapid water exchange for NH₃ groups. In the case of the HISQC, ¹⁵N transverse coherence is forced to be in-phase with respect to ¹H during the t_1 (¹⁵N)-evolution period by the ¹H WALTZ-16 decoupling sequence. As long as the in-phase term is kept, there is no contribution from scalar relaxation to ¹⁵N relaxation.⁷ Thus, for the HISQC experiment, ¹⁵N transverse relaxation during the t_1 -evolution period is determined by the R_2^{slow} and R_2^{fast} rates rather than the R_2^{in} and R_2^{out} rates, and is therefore independent of water exchange. In the HSQC experiment, on the other hand, ¹⁵N transverse coherence starts and ends as $2N_yH_z$ and during the t_1 -evolution period antiphase terms with respect to ¹H, such as $4N_xH_zH_z$ and $8N_yH_zH_zH_z$, are present. Transverse relaxation in the ¹⁵N-dimension of the HSQC is therefore characterized by the R_2^{in} and R_2^{out} rates, which are governed by rapid water-exchange for the NH₃ group. This effect results in significantly broader ¹⁵N line shapes for the NH₃ cross-peaks in the HSQC spectrum. Indeed, the ¹⁵N line shapes for the cross-peaks of the Lys3 and Lys55 NH₃ groups, both of which exhibit large $k_{\text{ex}}^{\text{water}}$ exchange rates (Figure 7c), are broader in the HSQC spectrum (Figure 5b) and consequently the sensitivity improvement for these cross-peaks in the HISQC spectrum (Figure 5c) is even more dramatic than that for the

(38) Hwang, T. L.; Mori, S.; Shaka, A. J.; van Zijl, P. C. M. *J. Am. Chem. Soc.* **1997**, *119*, 6203–6204.

(39) Hwang, T. L.; van Zijl, P. C. M.; Mori, S. *J. Biomol. NMR* **1998**, *11*, 221–226.

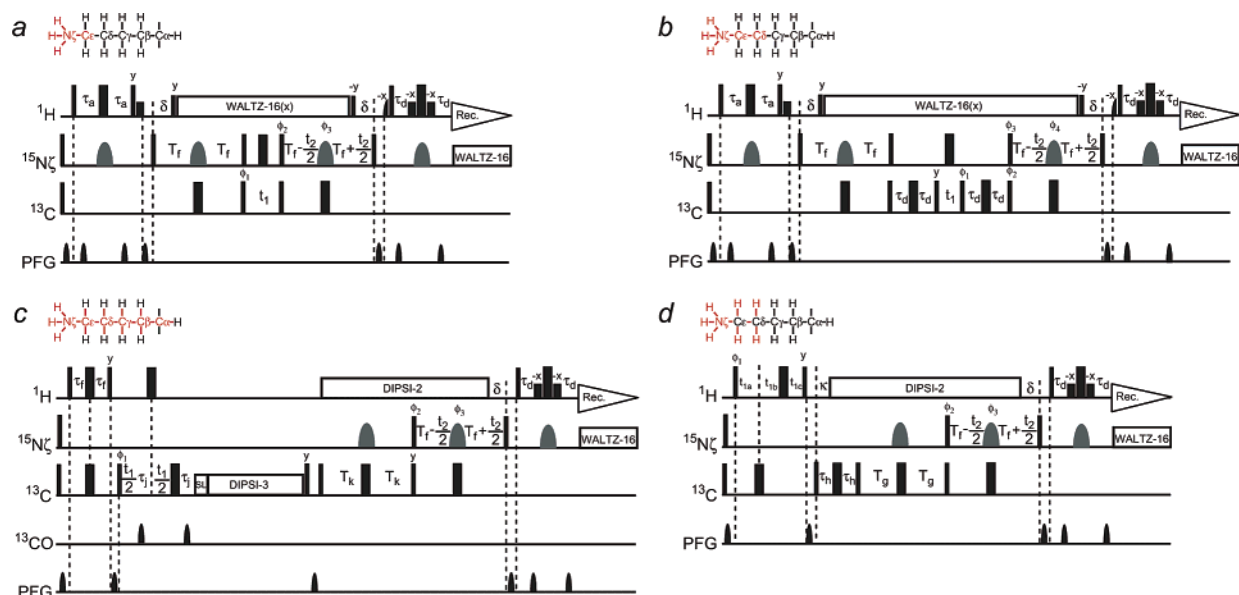


Figure 10. Suite of four 3D triple resonance experiments for the assignment of the ^1H and ^{15}N resonances of Lys NH_3 groups: (a) H_3NCE , (b) H_3NCECD , (c) $(\text{H})\text{CCENH}_3$, and (d) $\text{HDHE}(\text{CDCE})\text{NH}_3$. Correlations observed along a lysine side chain for each experiment are indicated in red above the pulse sequences. Bars and shapes representing pulses are as defined in Figure 4. ^1H composite pulses are applied with $\gamma B_1/2\pi = 3.3$ kHz. Delays commonly used in these experiments are: $\tau_a = 2.7$ ms; $\delta = 2.6$ ms; and $T_f = 45$ ms. Gradients were optimized to minimize the water signal. (a) 3D H_3NCE experiment. Hard ^{13}C pulses are applied with $\gamma B_1/2\pi = 17$ kHz. Phase cycles are $\phi_1 = \{x, -x\}$; $\phi_2 = \{2x, 2(-x)\}$; $\phi_3 = x$; rec. = $\{x, 2(-x), x\}$. Phases for states-TPPI are ϕ_1 and ϕ_2 for the ^{13}C and ^{15}N dimensions, respectively. (b) 3D H_3NCECD experiment. The delay τ_d was set to 3.3 ms to observe both ^{13}C and $^{13}\text{C}\delta$. Phase cycles are $\phi_1 = \{2y, 2(-y)\}$; $\phi_2 = \{2x, 2(-x)\}$; $\phi_3 = \{x, -x\}$; $\phi_4 = \{4x, 4y\}$; rec. = $\{x, 2(-x), x, -x, 2x, -x\}$. Phases for states-TPPI are ϕ_1 and ϕ_2 for the ^{13}C and ^{15}N dimensions, respectively. (c) 3D $(\text{H})\text{CCENH}_3$ experiment. A ^{13}C DIPSI-3⁵³ pulse train along y was applied at 43 ppm with $\gamma B_1/2\pi = 7.1$ kHz (mixing time, 23 ms). Prior to the DIPSI-3 pulse train, a ^{13}C spin-lock (1 ms) is applied along x . Delays are $\tau_f = 1.6$ ms; $\tau_j = 1.1$ ms; and $T_k = 14.3$ ms. Phase cycles are $\phi_1 = \{x, -x\}$; $\phi_2 = \{2x, 2(-x)\}$; $\phi_3 = \{4x, 4y\}$; rec. = $\{x, 2(-x), x, -x, 2x, -x\}$. Phases for states-TPPI are ϕ_1 and ϕ_2 for the ^{13}C and ^{15}N dimensions, respectively. (d) 3D $\text{HDHE}(\text{CDCE})\text{NH}_3$ experiment. Delays are $\tau_h = 3.3$ ms; $\kappa = 1.8$ ms; and $T_g = 17.6$ ms. Acquisition for the indirect ^1H dimension was achieved with a semiconstant time scheme²⁶ with t_{1a} , t_{1b} , and t_{1c} satisfying the relationships $(t_{1a} + t_{1b} - t_{1c}) = t_1$ and $(t_{1a} - t_{1b} + t_{1c}) = 3.2$ ms. Phase cycles are $\phi_1 = \{x, -x\}$; $\phi_2 = \{2x, 2(-x)\}$; $\phi_3 = \{4x, 4y\}$; rec. = $\{x, 2(-x), x, -x, 2x, -x\}$. Phases for states-TPPI are ϕ_1 and ϕ_2 for the ^1H and ^{15}N dimensions, respectively.

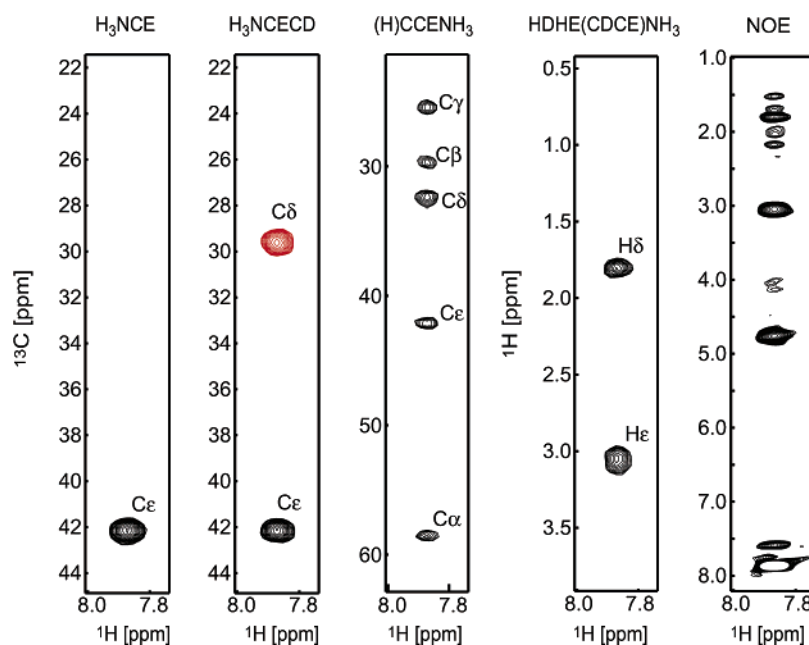


Figure 11. 2D slices taken from the four 3D NH_3 -selective triple resonance experiments illustrating correlations observed for the NH_3 group of Lys57. The pulse sequences for the triple resonance through-bond correlation experiments are those shown in Figure 10. The NOE spectrum was recorded using a 2D ^1H – ^1H NOE experiment in which the NOE component is followed by a NH_3 -selective HMQC scheme (using ^{15}N 90° E-BURP2 pulses to selectively excite the NH_3 region) without ^{15}N evolution. All spectra were recorded on the $^{15}\text{N}/^{13}\text{C}$ -labeled HOXD9 homeodomain–DNA complex at 25°C at a ^1H frequency of 500 MHz.

cross-peak of Lys57 which exhibits the slowest $k_{\text{ex}}^{\text{water}}$ exchange rate.

To understand the ^{15}N relaxation process in the HISQC experiment, we analyzed ^{15}N transverse relaxation for the in-

phase single quantum term N_x using the pulse sequence shown Figure 8a. The relaxation rates, referred to as $R_2^{\text{app}}(N_x)$, were obtained from a single-exponential fit to the initial decay (Figure 8b,c). This analysis is only meaningful in a phenomenological sense, since theoretically the relaxation process should be biexponential and given by

$$I(T) = I(0)\{a_{\text{in}} \exp(-R_2^{\text{slow}}T) + a_{\text{out}} \exp(-R_2^{\text{fast}}T)\} \quad (8)$$

where a_{in} and a_{out} represent the populations of the inner and outer components at time zero. (Note that R_2^{slow} and R_2^{fast} rather than R_2^{in} and R_2^{out} are included because N_x is independent of scalar relaxation). In practice, accurate determination of rate constants using biexponential fitting is difficult as pointed out previously.^{30,31} The apparent transverse relaxation rate from the initial slope is given by $a_{\text{in}}R_2^{\text{slow}} + a_{\text{out}}R_2^{\text{fast}}$. For the pulse sequence in Figure 8a, values of a_{in} and a_{out} should be close to 0.25 and 0.75, respectively, but will depend on the experimental conditions such as the delay τ_b .³⁰ For Lys57 NH₃, the value of $0.25R_2^{\text{slow}} + 0.75R_2^{\text{fast}}$ is calculated to be $3.8 \pm 0.32 \text{ s}^{-1}$ at 35 °C and $3.3 \pm 0.09 \text{ s}^{-1}$ at 25 °C (Table 1). These values are reasonably close to those obtained for $R_2^{\text{app}}(N_x)$: $4.45 \pm 0.15 \text{ s}^{-1}$ at 35 °C and $4.41 \pm 0.10 \text{ s}^{-1}$ at 25 °C. Thus, ¹⁵N transverse relaxation of the in-phase terms that are exclusively observed in the HISQC experiment is indeed independent of scalar relaxation owing to water exchange and, therefore, significantly slower.

Triple Resonance NMR Experiments for Assignment of Lys NH₃. The ¹J-coupling between ¹⁵Nζ and ¹³Cε of lysine residues were measured using the spin-echo difference constant-time ¹H-¹⁵N HSQC experiment shown in Figure 9a. In this experiment, the ¹H-composite decoupling pulses applied after the delay δ maintain ¹⁵N in-phase terms during the 2T_d period, ensuring high sensitivity through the elimination of scalar relaxation during the ¹⁵N-chemical shift evolution period. The measured ¹J_{CN} values range from 4.7 to 5.0 Hz (Figure 9b) and are considerably smaller than the ¹J_{CαN} coupling between backbone ¹⁵N and ¹³Cα (9–11 Hz).⁴¹

We designed a suite of triple resonance NMR experiments for through-bond correlations between ¹⁵NH₃ and other ¹H and ¹³C resonances within a lysine residue (Figure 10). The four pulse sequences termed H₃NCE, H₃NCECD, (H)CCENH₃, HDHE(CDCE)NH₃ experiments (Figure 10, parts a, b, c, and d, respectively) are equivalent to HNCA,⁴⁰ HNCACB,⁴² (H)CNH,⁴³ and HBHA(CBCA)NH₃⁴⁴ experiments, respectively, but optimized for NH₃ groups. Because of the ¹⁵N relaxation properties of the NH₃ group described above, these experiments were designed to keep ¹⁵N transverse magnetization in-phase with respect to ¹H as long as possible. While Grzesiek and Bax originally proposed a similar concept for experiments involving the backbone amide group,⁴⁰ it is critically important for NH₃. Since the new experiments make use of a relatively small ¹J_{CN} between ¹⁵Nζ and ¹³Cε (4.7–5.0 Hz), the coherence transfer requires a longer period for ¹⁵N transverse magnetization than the corresponding experiments for backbone amide groups.

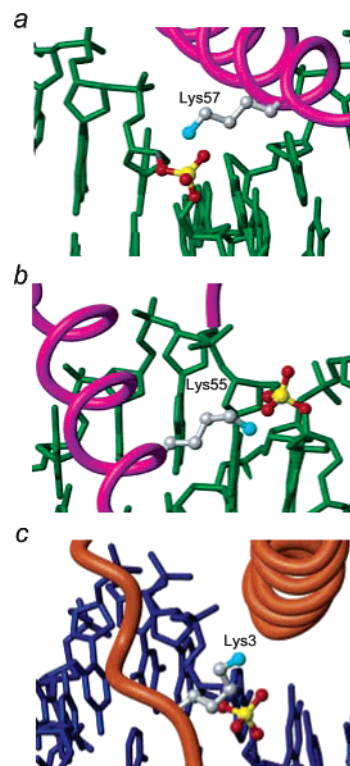


Figure 12. Location of the observed lysine NH₃ groups in the crystal structures of homeodomain–DNA complexes. Lysine residues and interacting DNA–phosphate groups are depicted as ball-and-sticks. All lysine NH₃ groups observed in the present study interact with a DNA phosphate group. Panels a and b show the interaction of Lys57 and Lys55, respectively, with a DNA–phosphate group seen in the crystal structure of the engrailed homeodomain–DNA complex (PDB accession code 3HDD).⁴⁵ These two lysine residues are conserved among the Q50-class homeodomains.^{45,46} Panel c illustrates the interaction of Lys3 with a DNA–phosphate group seen in the crystal structure of the Msx-1 homeodomain–DNA complex (PDB entry 1IG7).⁴⁷ Lys3 is less well conserved than the other two lysine residues and is only observed in the crystal structure of the Msx-1 homeodomain–DNA complex. The intermolecular N⋯O distances between the NH₃ and DNA phosphate groups are 3.2 and 2.9 Å for Lys55 and Lys57, respectively, consistent with the presence of intermolecular hydrogen bonds or salt bridges. Although the distance between Lys3 NH₃ and a DNA phosphate group is 5.4 Å, a simple rotation about the χ₃ side-chain torsion angle can readily reduce this distance to less than 3.0 Å.

However, these experiments for NH₃ groups are intrinsically sensitive owing to very slow relaxation of in-phase ¹⁵N transverse magnetization that satisfies the condition $(2^1J_{\text{CN}})^{-1} < R_2(N_x)^{-1}$. Figure 11 illustrates spectra recorded with these pulse sequences. Using the triple resonance data and lysine ¹H and ¹³C resonances that had been assigned in a previous study,¹² we were able to assign the NH₃ signals seen in the HISQC spectrum to Lys3, Lys55, and Lys57 as shown in Figure 5c.

Observed Lys NH₃ Groups Are Involved in Interaction with DNA. The locations of the NH₃ groups of Lys3, Lys55, and Lys57 in the crystal structures of homeodomain–DNA complexes are shown in Figure 12. While the crystal structure of the HOXD9 homeodomain–DNA complex has not been determined, crystal structures of other homeodomain–DNA complexes that are highly homologous to the present system are available,^{45–47} and our previous NMR studies have shown

(40) Grzesiek, S.; Bax, A. *J. Magn. Reson.* **1992**, *96*, 432–440.

(41) Delaglio, F.; Torchia, D. A.; Bax, A. *J. Biomol. NMR* **1991**, *1*, 439–446.

(42) Wittekind, M.; Mueller, L. *J. Magn. Reson., Ser. B* **1993**, *101*, 201–205.

(43) Logan, T. M.; Olejniczak, E. T.; Xu, R. X.; Fesik, S. W. *FEBS Lett.* **1992**, *314*, 413–418.

(44) Wang, A. C.; Lodi, P. J.; Qin, J.; Vuister, G. W.; Gronenborn, A. M.; Clore, G. M. *J. Magn. Reson., Ser. B* **1994**, *105*, 196–198.

(45) Fraenkel, E.; Rould, M. A.; Chambers, K. A.; Pabo, C. O. *J. Mol. Biol.* **1998**, *284*, 351–361.

(46) Fraenkel, E.; Pabo, C. O. *Nat. Struct. Biol.* **1998**, *5*, 692–697.

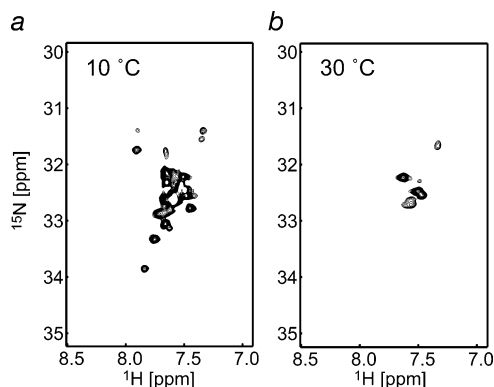


Figure 13. NH_3 -selective HISQC spectra of the 128 kDa ^{15}N -labeled enzyme I dimer (2×579 residues) from *Thermoanaerobacter tengcongensis* recorded at (a) 10 °C and (b) 30 °C. The NMR sample contained 0.4 mM enzyme I dissolved in 20 mM sodium acetate (pH 5.5), 0.1 mM NaN_3 , and 2 mM DTT. Note that the sample is not deuterated. The experiments were recorded at 800 MHz using the pulse sequence shown in Figure 4c. Enzyme I contains 54 lysine residues, of which seven are involved in salt-bridge interactions with glutamate or aspartate residues in the crystal structures.^{50–52} Cross-peaks observed at 30 °C are likely to arise from these NH_3 groups owing to protection against rapid water exchange.

that the structure and mode of HOXD9 homeodomain binding to DNA is essentially the same.¹² In the crystal structures, the NH_3 groups of Lys55 and Lys57 form hydrogen bonds with DNA phosphate groups ($\text{N}\cdots\text{O}$ distances: 3.2 Å for Lys55; 2.9 Å for Lys57). Only the crystal structure of the Msx-1 homeodomain–DNA complex⁴⁷ contains coordinates of Lys3, and it is also close to a DNA phosphate group. These results indicate that lysine NH_3 groups involved in hydrogen bonding/salt bridge interactions are easier to observe since they are partially protected from rapid water exchange. (Note, while water exchange does not affect in-phase ^{15}N transverse relaxation it does cause significant line broadening in the ^1H dimension). This unique feature allows for selective observation of NH_3 groups involved in functional interactions, simply by adjusting pH and temperature.

Potential Use of Lys NH_3 as an Alternative Probe for Very Large Systems. Recently Kay and co-workers have demonstrated that CH_3 groups in an otherwise deuterated background are sensitive probes that can be analyzed for systems larger than 100 kDa.^{9,10,48} For the same S_{axis}^2 and τ_r , relaxation of in-phase ^{15}N transverse coherence for an NH_3 group should be intrinsically slower than ^{13}C relaxation for a CH_3 group owing to the smaller nuclear gyromagnetic ratio of ^{15}N relative to ^{13}C . Thus, if water exchange is slow, lysine NH_3 groups could potentially provide alternative probes for very large systems.

We tested this hypothesis using the 128 kDa dimer of ^{15}N -labeled enzyme I at pH 5.5. HISQC spectra were measured at 10 and 30 °C (Figure 13). The water-exchange rates at 10 °C are expected to be ~ 9 -fold slower than those at 30 °C.⁴⁹ Since

the value of the exchange rate at pH 5.5 and 10 °C is $\sim 15 \text{ s}^{-1}$ for the NH_3 group of a free lysine,⁴ observation of many NH_3 groups is feasible. Indeed, although the protein was not deuterated, many cross-peaks arising from NH_3 groups of the 128 kDa enzyme I (54 lysine residues per monomer) were observed at 10 °C, of which ~ 10 cross-peaks are isolated from the main cluster within the range of ^{15}N chemical shifts between 31 and 34 ppm. At 30 °C, on the other hand, only ~ 6 signals were observed because of the rapid water-exchange rates. The available crystal structures of enzyme I suggest that seven lysine residues make salt bridges with glutamate or aspartate carboxylate groups, with $\text{N}\cdots\text{O}$ distances shorter than 3.2 Å.^{50–52} The lysine NH_3 signals observed at 30 °C are likely to arise from these residues.

Concluding Remarks. In this paper, we have described various aspects of heteronuclear ^1H – ^{15}N NMR spectroscopy for lysine NH_3 groups in proteins. In this study, ^{15}N resonances for lysine NH_3 groups were found to be located between 31 and 34 ppm. Even if the water-exchange rate is slow enough to permit observation of the proton NH_3 resonances by 1D ^1H NMR, ^1H – ^{15}N cross-peaks arising from NH_3 groups are rarely observed in a conventional HSQC experiment typically employed for backbone amide groups owing to the limited rf strength available for ^{15}N pulses and severely broadened ^{15}N line shapes. The ^{15}N transverse relaxation properties of the NH_3 group are unique in that they are highly affected by rapid water exchange via a mechanism that can be attributed to scalar relaxation of the second kind. As a consequence, neither HMQC nor HSQC experiments are optimal for the observation of NH_3 correlations. In the latter experiments, ^{15}N line shapes of the NH_3 cross-peaks are even broader than those of backbone amide groups, although the intrinsic ^{15}N relaxation rates of NH_3 are much slower. The HISQC experiment presented here is not affected by scalar relaxation in the ^{15}N dimension and therefore provides strikingly better resolution in the ^{15}N dimension and much higher sensitivity for detection of NH_3 correlations than either HSQC or HMQC experiments. Since ^{15}N relaxation of in-phase terms is very slow, heteronuclear NMR experiments for Lys NH_3 groups can be highly sensitive as long as the in-phase terms are maintained. Triple resonance experiments that implement this principle offer a useful means for assignment of lysine NH_3 groups. Because of their favorable ^{15}N relaxation properties, lysine NH_3 groups offer alternative probes to methyl groups for studies involving systems in excess of 100 kDa, as demonstrated by the data obtained for the 128 kDa enzyme I dimer. For studies on protein–DNA complexes, the lysine NH_3 cross-peaks observed at 35 °C are confined to those involved in direct interactions with DNA-phosphate groups. Indeed, because water exchange for NH_3 groups involved in functional interactions (i.e., hydrogen bonds or salt bridges) tends to be slow (i.e., the protons are protected from exchange) such lysine NH_3 groups are easier to characterize by heteronuclear NMR.

Acknowledgment. We thank Ad Bax and Dennis Torchia for useful discussions and Jun Hu for suggesting the use of a coaxial NMR tube. This work was supported by funds from the Intramural Program of the NIH and NIDDK and in part by the AIDS Targeted Antiviral program of the Office of the Director of the NIH (to G.M.C.).

JA0683436

(47) Hovde, S.; Abate-Shen, C.; Geiger, J. H. *Biochemistry* **2001**, *40*, 12013–12021.

(48) Sprangers, R.; Gribun, A.; Hwang, P. M.; Houry, W. A.; Kay, L. E. *Proc. Natl. Acad. Sci. U.S.A.* **2005**, *102*, 16678–16683.

(49) Englander, S. W.; Downer, N. W.; Teitelbaum, H. *Annu. Rev. Biochem.* **1972**, *41*, 903–924.

(50) Oberholzer, A. E.; Bumann, M.; Schneider, P.; Bachler, C.; Siebold, C.; Baumann, U.; Erni, B. *J. Mol. Biol.* **2005**, *346*, 521–532.

(51) Marquez, J.; Reinelt, S.; Koch, B.; Engelmann, R.; Hengstenberg, W.; Scheffzek, K. *J. Biol. Chem.* **2006**, *281*, 32508–32513.

(52) Teplyakov, A.; Lim, K.; Zhu, P. P.; Kapadia, G.; Chen, C. C.; Schwartz, J.; Howard, A.; Reddy, P. T.; Peterkofsky, A.; Herzberg, O. *Proc. Natl. Acad. Sci. U.S.A.* **2006**, *103*, 16218–16223.

(53) Shaka, A. J.; Lee, C. J.; Pine, A. *J. Magn. Reson.* **1988**, *77*, 274–293.